8

Predicting Macroscale Effects Through Nanoscale Features

Victor J. Bellitto[1] and Mikhail I. Melnik[2]
[1]*Naval Surface Warfare Center*
[2]*School of Engineering Technology,*
Southern Polytechnic State University, Marietta, GA
USA

1. Intoduction

Atomic force microscopy is extremely useful in the study of surface defects in crystals by providing topographical data at the nanometric scale. With the aide of advanced statistical analysis, nanoscale surface data acquired through atomic force microscopy can also be utilized to predict behavior at the macroscale. The behavioral model presented is the measure of shock sensitivity required to produce detonation of explosive crystal test samples. The surfaces studied were of 7 different varieties of (RDX) crystalline explosives from 5 manufacturers (Doherty & Watts, 2008). It has been speculated that particle size, crystal defects, density and crystal morphology may play a role in the shock sensitivity of RDX and there have been numerous attempts to quantify and/or link particular features of the explosive particles to the shock sensitivity behavior of their larger compositions (Doherty and Watts, 2008). The shock sensitivity data were obtained from model test compositions prepared as polymer-bonded explosives using hydroxy-terminated polybutadiene (HTPB) as the binder. The shock sensitivity, measured in a gap test, is the shock required to produce a detonation of the test composition 50% of the time. Varied card thicknesses of poly(methyl-methacrylate) (PMMA) are used to attenuate the initiating charge entering the sample tube. The shock pressure (GPa) impacting the sample is determined by the number of cards. A small number of cards translate to a larger shock and thus a less shock sensitive sample.

2. Experimental

The AFM analysis of the RDX crystal surfaces was performed using a Multimode V scanning probe microscope (Veeco Metrology Group). The instrument was operated in Tapping Mode, where topographical analysis is performed with minimal contact of the surface. The crystal topography is mapped by lightly tapping the surface with an oscillating probe tip. The sample surface topography modifies the cantilever's oscillation amplitude and the topography image is obtained by monitoring these changes while closing the z feedback loop to minimize them. A first order algorithm supplied by Veeco was used to "flatten" the images. The flatten command modifies the scanned image removing tilt and thus leveling the image.

A variety of surface features were observed including edge and screw dislocations, voids, cracks, peaks, valleys, plateaus, etc. Examples of images acquired of the RDX particles surfaces are shown in Fig. 1-7. They are presented as amplitude images since they more easily display the shape of the sample surface. The amplitude image is equivalent to a map of the slope of the sample. The z-scale shows the tip deflection as it encountered sample topography. The amplitude image on harder samples better highlights the edges of features while on softer samples it can depict subsurface features better than the topography image.

The root mean square (*RMS*) calculation (R) of the surface imagery acquired in height mode was used to determine the roughness and to quantify the different surface topologies. The roughness was calculated by finding the median surface height for the scanned image and then evaluating the standard deviation. The equation for determining the surface roughness is

$$R = \left(\frac{1}{MN} \sum_{k=0}^{M-1} \sum_{l=0}^{N-1} \left[z(x_k, y_l) - \mu \right]^2 \right)^{0.5},$$

where μ is the mean value of the height, *z*, across in-plane coordinates *(x,y)*:

$$\mu = \frac{1}{MN} \sum_{k=0}^{M-1} \sum_{l=0}^{N-1} z(x_k, y_l).$$

The necessity to add objectivity to the consistency across the surface is demonstrated by Fig. 1-7. Although the side by side images obtained are from the same particle they demonstrate two very different surface morphologies and/or different roughness measurements.

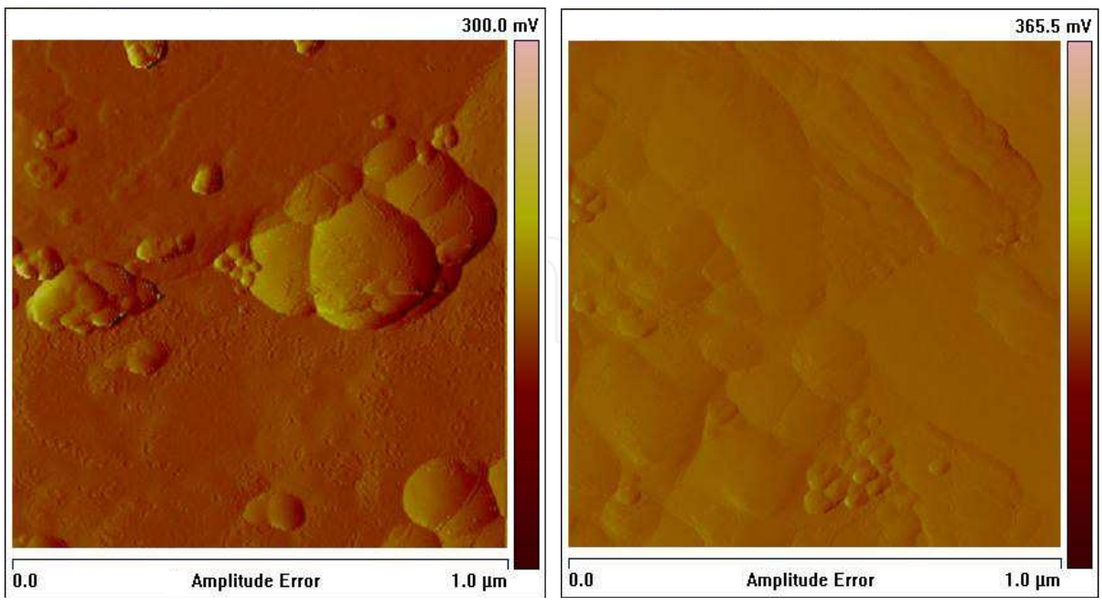

Fig. 1. AFM scan images obtained from the same particle of material I. A roughness measurement of 18.9 nm was obtained for image on the left while 29.6 nm was obtained for image on the right.

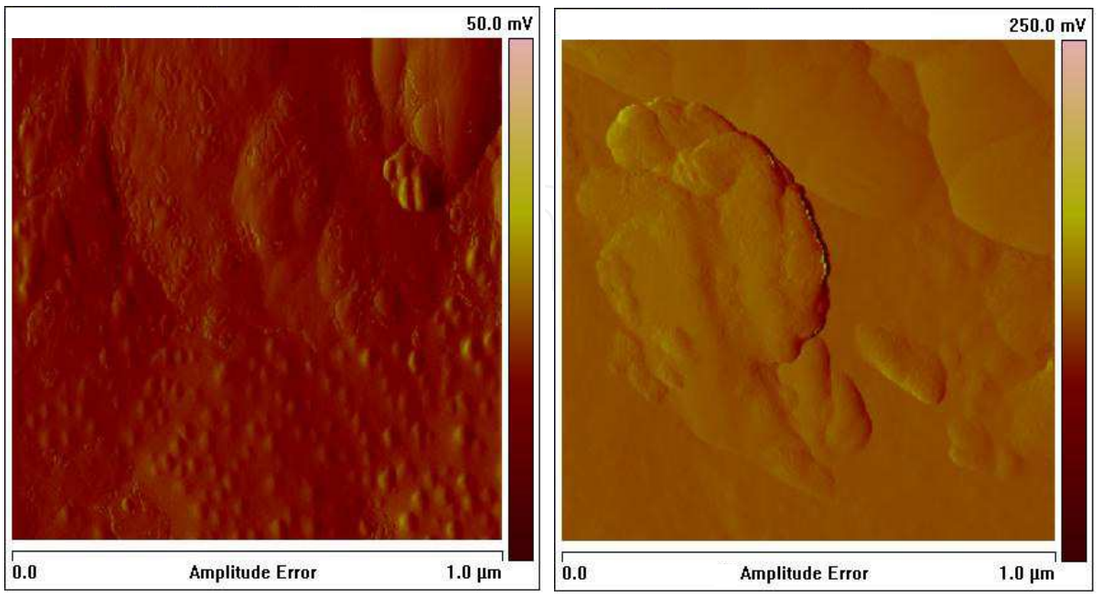

Fig. 2. AFM scan images obtained from the same particle of material II. A roughness measurement of 9.81 nm was obtained for image on the left while 24.4 nm was obtained for image on the right.

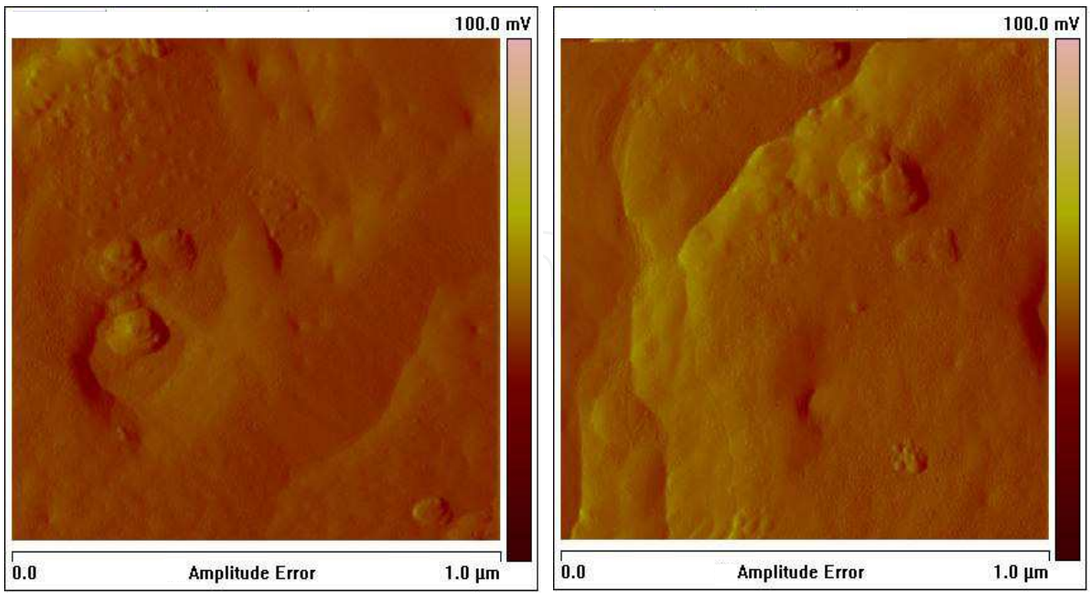

Fig. 3. AFM scan images obtained from the same particle of material III. A roughness measurement of 9.31 nm was obtained for image on the left while 21.5 nm was obtained for image on the right.

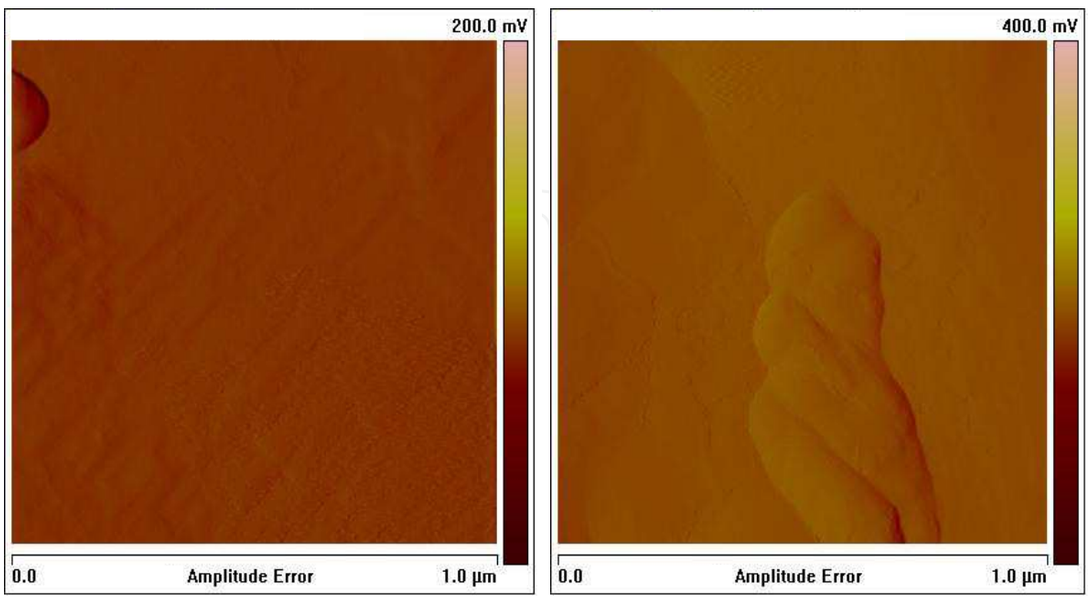

Fig. 4. AFM scan images obtained from the same particle of material IV. A roughness measurement of 5.05 nm was obtained for image on the left while 20.9 nm was obtained for image on the right.

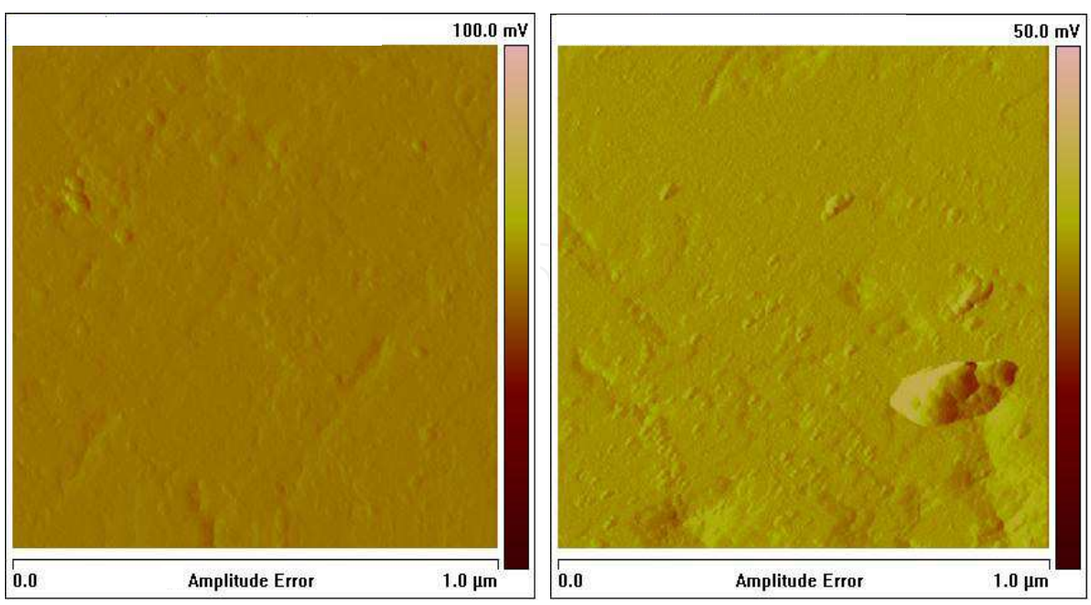

Fig. 5. AFM scan images obtained from the same particle of material V. A roughness measurement of 1.07 nm was obtained for image on the left while 3.7 nm was obtained for image on the right.

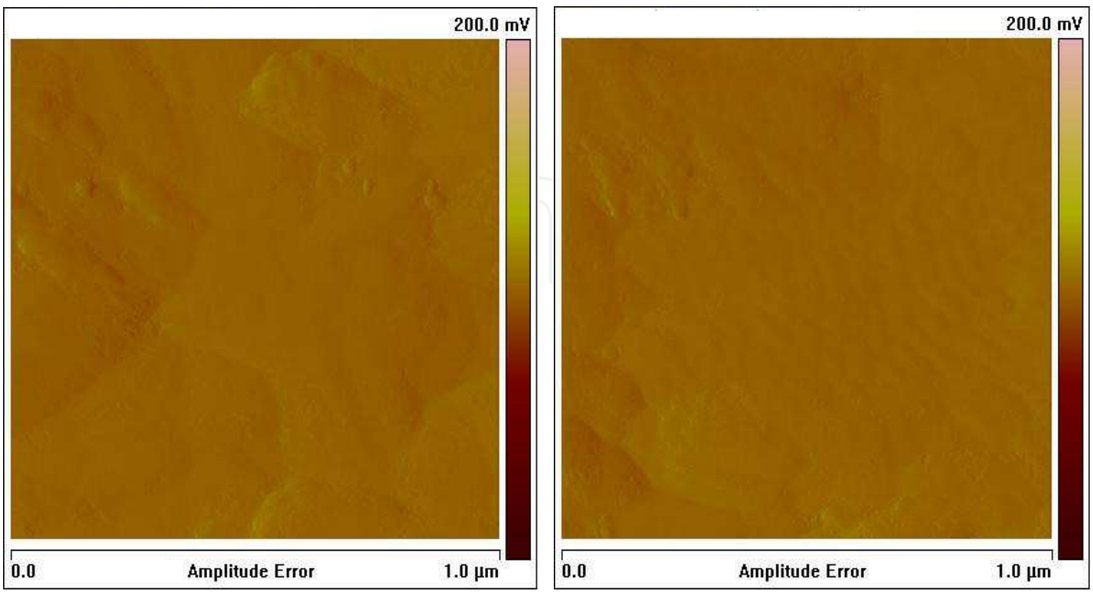

Fig. 6. AFM scan images obtained from the same particle of material VI. A roughness measurement of 1.07 nm was obtained for image on the left while 3.7 nm was obtained for image on the right.

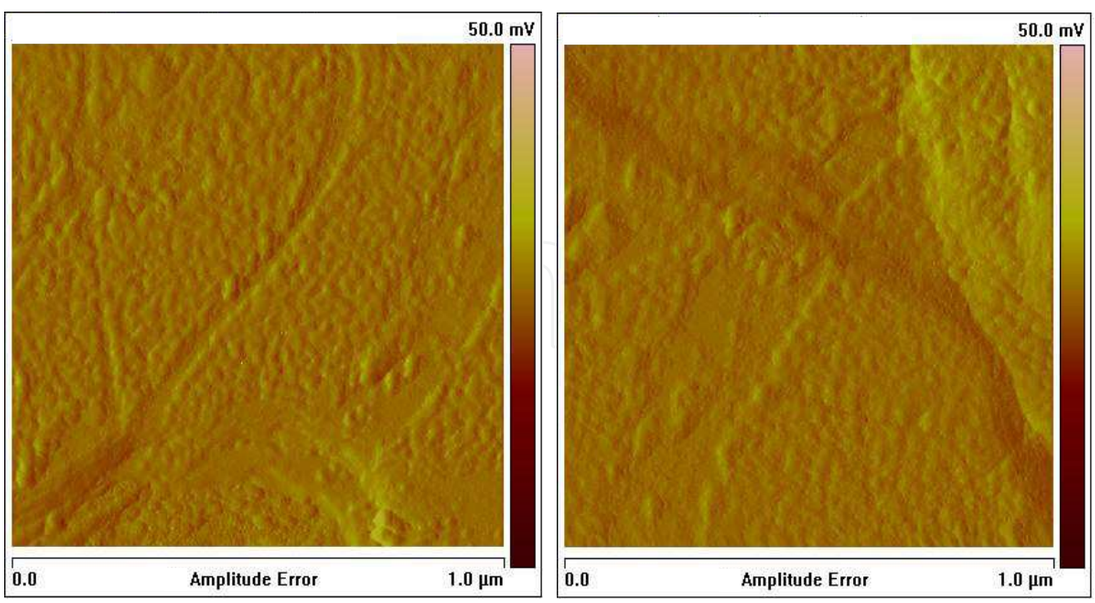

Fig. 7. AFM scan images obtained from the same particle of material VII. A roughness measurement of 2.9 nm was obtained for image on the left while 4.69 nm was obtained for image on the right.

3. Statistical analysis

Statistical analysis can generally be subdivided into three steps or sections. The first step involves obtaining the data and constructing the relevant variables. The second involves some basic statistical investigations, such as correlations between the variables or in the case of multiple sample comparisons, hypothesis testing. Often the first two steps may be sufficient, but in the event that the research requires an understanding of the exact relationships between the various variables, the quantitative effects one variable has on another, a further step in the form of a regression analysis becomes necessary. The discussion below outlines the steps encompassed in the statistical analysis.

3.1 Data and the construction of variables

The AFM data consist of individual 1 μm² surface scans obtained from seven different RDX materials. Each scan produces one observation that contains the information on the actual surface variation, roughness of the area of the scan, R (RMS). The scans were taken from seven different materials, however, each material is comprised of particles, and differences between particles of the same material in terms of their surface characteristics are possible. Therefore, five particles of each material were selected at random and 5-6 scans of different regions of the surface of each particle were acquired.

This approach allows modeling of the surface heterogeneity between the seven materials in three possible ways: the average measure of observed surface roughness, the variability between the particles, and lastly the variation in the surface roughness across the surface of a particle. For further discussion see Bellitto & Melnik (2010) and Bellitto et al (2010).

Multiple scans per particle allow the construction of two measures of the surface characteristics of the particle, the particle average (R_{pm}),

$$R_{pm} = \frac{1}{n}\sum_{s=1}^{n} R_{pms}$$

and the particle standard deviation (S_{pm}),

$$S_{pm} = \left(\frac{1}{n-1}\sum_{s=1}^{n} (R_{pms} - R_{pm})^2 \right)^{0.5},$$

where the subscript p refers to the particle and m to the material. The subscript s refers to the individual scan and n is the number of scans per particle. Thus, R_{pm} represents the average value of all scans for that particle and S_{pm} represents the standard deviation of roughness for that particle. These statistics are listed in Table 1.

Shown in Table 1 are the particle average (R_{pm}) and the particle standard deviation (S_{pm}) values. These are limited to describing the individual particle characteristics but they can be used to construct variables describing the material characteristics. R_{pm} can simply be averaged to construct the average measure of observed surface roughness of the material (R_m),

		Particle Level Data		Material Level Data		
Material	Particle	Rpm	Spm	Rm	Sm	Smμ
I	1	19.100	6.531	18.270	4.131	5.929
	2	14.617	1.994			
	3	10.128	3.229			
	4	23.467	3.704			
	5	24.040	5.198			
II	1	10.518	7.730	8.425	4.853	6.120
	2	18.268	7.614			
	3	5.062	4.247			
	4	3.653	2.417			
	5	4.624	2.255			
III	1	13.794	8.236	16.040	11.033	7.457
	2	7.014	3.723			
	3	25.006	16.742			
	4	22.335	17.346			
	5	12.052	9.121			
IV	1	11.255	12.770	10.565	9.807	4.310
	2	4.872	3.160			
	3	10.220	11.350			
	4	16.912	17.749			
	5	9.564	4.007			
V	1	2.000	1.619	5.322	3.622	3.165
	2	6.207	1.698			
	3	10.244	7.900			
	4	3.396	4.034			
	5	4.762	2.856			
VI	1	15.740	4.633	10.067	3.612	4.784
	2	13.982	3.868			
	3	7.934	2.370			
	4	8.753	5.830			
	5	3.923	1.358			
VII	1	10.335	3.462	6.150	2.877	5.278
	2	5.120	2.169			
	3	12.820	7.432			
	4	1.482	1.041			
	5	0.994	0.281			

Table 1. Construction of Measures of Surface Roughness

$$R_m = \frac{1}{N}\sum_{p=1}^{N} R_{pm} \ ,$$

where N represents the number of particles for the material. Similarly, the average measure of particle standard deviation can be constructed,

$$S_m = \frac{1}{N}\sum_{p=1}^{N} S_{pm} \ .$$

This simple average measure accounts for the average variability in the surface roughness across the particle surface.

At this point two measures of surface roughness and its variability have been constructed. One is the particle average level for the material (R_m) and the other is the average variation in surface roughness across the particle surface (S_m). To quantify the variation between particles the standard deviation of the distribution of R_{pm}, is introduced and expressed as

$$S_{m\mu} = \left(\frac{1}{N-1}\sum_{p=1}^{N} (R_{pm} - R_m)^2 \right)^{0.5} \ .$$

This measure enables us to account for the heterogeneity between the various particles of the material.

Cyclotetramethylene-tetranitramine (HMX), a major impurity within RDX, has been reported to be as high as 17% (Doherty & Watts, 2008). Table 2 provides a basic summary of the shock sensitivity of the seven materials and the mean % of HMX impurity. The HMX impurity is included since impurities can significantly alter the periodicity of a crystal and thus affect its surface roughness.

Material	Impurity (Mean % HMX)	Sensitivity (GPa)
I	7.36	4.2
II	0.02	4.66
III	0.03	2.21
IV	8.55	3.86
V	0.82	5.24
VI	0.02	5.21
VII	0.19	5.06

Table 2. Impurity (%HMX) and shock sensitivity (GPa) of the materials used in our study.

3.2 Basic comparison of the materials

The average surface roughnesses of the materials, shown in Table 1, are first compared using analysis of variance (ANOVA). ANOVA is a statistical method used to compare population characteristics for multiple populations. ANOVA relies on three important assumptions, randomness and independence, normality, and homogeneity of variances. As discussed previously, our process of particle selection met the assumption of randomness. The Shapiro-

Wilk test is employed to test for normality, to test if the underlying population can be assumed to be normally distributed. Table 3 presents the results of the test for the particle (R_{pm}) values for all seven samples (materials). The Shapiro-Wilk test fails to reject the null hypothesis of normality with p=0.10 for all of the samples. The null hypothesis assumes that the underlying population is normally distributed. If the test fails to reject the null hypothesis then that indicates that the assumption of the underlying population being normally distributed cannot be disproved. However, the Shapiro-Wilk test may at times be misleading and a visual examination of the data may be recommended. Interestingly enough, the F test used in ANOVA is relatively robust against the assumption of normality (Levine et al, 2010), but the assumption of homogeneity of variances is crucial to the validity of the test.

Material	W	V	z	Prob>z
I	0.921	0.929	-0.097	0.538
II	0.828	2.032	1.107	0.134
III	0.937	0.739	-0.379	0.648
IV	0.952	0.565	-0.682	0.752
V	0.946	0.634	-0.556	0.711
VI	0.948	0.617	-0.585	0.721
VII	0.897	1.218	0.273	0.392

Table 3. Results of Shapiro-Wilk test

The Levene test for homogeneity of variances is performed on the R_{pm} data and the groups are defined as the individual materials. The test compares multiple samples to determine if they are drawn from populations with equal variances. The value of the F statistic from the Levene test is 0.49367, while the critical value for the rejection of the null hypothesis of homogeneity of variances is 2.445259, the hypothesis of homogeneity of variances cannot be rejected by the test[1]. This enables us to perform the one way ANOVA on our R_{pm} data, grouped by their corresponding materials.

The ANOVA method enables us to check if there is enough statistical evidence to reject the hypothesis that the R_m values of the seven materials are statistically not different from each other. The ANOVA output is presented in Table 4 and it shows that the hypothesis of equal R_m values is rejected by the data.

The ANOVA results demonstrate that these materials differ substantially in terms of their particle average roughness.

The focus of our research is to investigate a possible connection between the surface roughness and the shock sensitivity of the material. One simple way in which this connection can be examined is with the help of correlations, see Table 5. A clear negative correlation is observed between the measure of shock sensitivity (GPa) and the three

[1] In the event the Levene test rejected the null hypothesis, we would not be able to proceed with ANOVA and would have to use weaker testing techniques such as the Kruskal-Wallis test. For further discussion on the Levene test please see Levine et al (2010).

SUMMARY

Groups	*Count*	*Sum*	*Average*	*Variance*
I	5	91.352	18.2704	35.15459
II	5	42.12567	8.425133	37.45042
III	5	80.20038	16.04008	55.60776
IV	5	52.823	10.5646	18.57295
V	5	26.60883	5.321767	10.01659
VI	5	50.33267	10.06653	22.88255
VII	5	30.7508	6.15016	27.86016

ANOVA

Source of Variation	*SS*	*df*	*MS*	*F*	*P-value*	*F crit*
Between Groups	705.2395	6	117.5399	3.964342	0.005398	2.445259
Within Groups	830.1801	28	29.64929			
Total	1535.42	34				

Table 4. ANOVA of Rpm

	%HMX	Sensitivity	Rm	Sm
Sensitivity	-0.181			
	-0.411			
Rm	0.448	**-0.694**		
	1.120	***-2.155***		
Sm	0.284	**-0.896**	0.452	
	0.662	***-4.518***	1.133	
Smμ	-0.170	**-0.706**	**0.656**	0.414
	-0.386	***-2.230***	***1.945***	1.016

Table 5. Correlations and their statistical significance

measures of surface roughness of the material. This demonstrates that higher levels of surface heterogeneity are associated with lower levels of shock sensitivity.

Furthermore, all of the correlation coefficients between the surface characteristics measures and the shock sensitivity are statistically significant at or above the 90% level of significance. The statistical significance of the coefficients is determined by their corresponding t values. The t statistics for the significance test of the correlation coefficients are reported in italics under their corresponding coefficient and those that are significant at or above the 90% level are highlighted in bold font. The test statistic is obtained by the equation

$$t = r\sqrt{\frac{N_m - 2}{1 - r^2}} \ ,$$

where r is the correlation coefficient and N_m is the number of observations, which in this case is limited to seven, the number of materials used in this study.

3.3 Regression analysis

Regression analysis is designed to establish numerical relationships between the regressors, the independent variables and the dependent variable. A multivariable regression enables one to interpret the regression coefficients as partial derivatives of the dependent variable with respect to the regressor. Various regression techniques exist, but given the simple setup of our problem the most basic model, the Ordinary Least Squares, can adequately serve the purpose. For further discussion of various regression techniques see Greene (2003). The greater concern is the fact that the data is limited to only seven materials and seven observations of shock sensitivity. Generally, regression techniques require satisfying the Central Limit Theorem requirements which demand a higher level of observations. Unfortunately, the data is limited by the number of materials available in the study.

The relationship between the surface roughness characteristics of the RDX materials and their shock sensitivity is investigated. A simple plot (Figure 8) shows that the shock sensitivity of the material is correlated with the level of surface roughness.

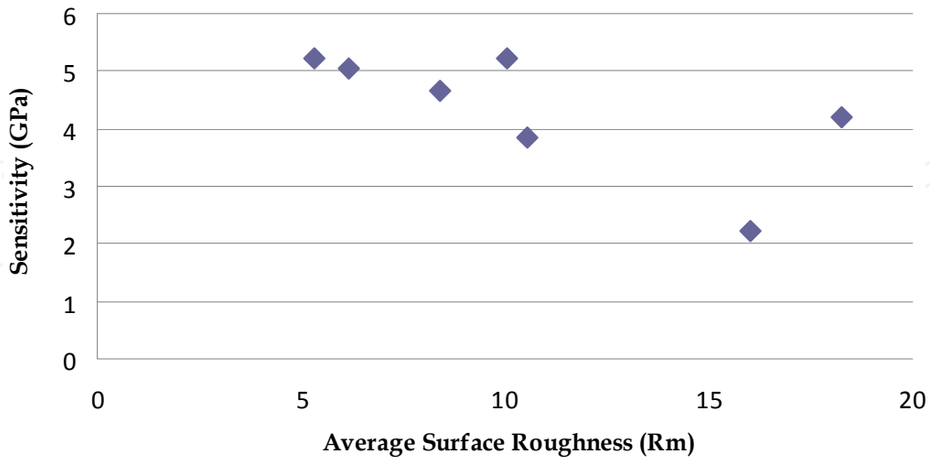

Fig. 8. Plot of sensitivity of material versus average surface roughness (Rm)

However, the plot also demonstrates that there is potential for heteroscedasticity in the data. Although heteroscedasticity does not create a bias in determining the regression coefficients themselves, the statistical significance of those coefficients becomes essentially unknown as

the standard errors become incorrectly computed by the basic OLS technique. To test for the presence of heteroscedasticity the Breusch-Pagan / Cook-Weisberg test is employed with the test statistics distributed as χ^2 with the degrees of freedom equal to the number of regressors. The Breusch-Pagan / Cook-Weisberg test for heteroscedasticity indicates $\chi^2(1)=3.71$, which corresponds to a probability > χ^2 = 0.0542. Thus, with a p value of less than 0.05 the test fails to reject the hypothesis of no heteroscedasticty, however with a p value near 0.1, the hypothesis of no heteroscedasticty is rejected. In an effort to be conservative in the analysis a value of p=0.1 is selected. The problem is further amplified by the fact that the sample size is very small (only seven observations of shock sensitivity), which reduces the robustness of the White/Huber estimator, a commonly used method for heteroscedasticity correction. As a result, the HCCM estimator known as HC3 is employed, this estimation technique was discussed by MacKinnon and White (1985), and was later shown to perform better than its alternatives in small samples, see Long and Ervin (2000).

The test shows that the relationship between shock sensitivity and S_m does not exhibit any heteroscedasticity. The Breusch-Pagan / Cook-Weisberg test provides $\chi^2(1)=1.73$, which corresponds to probability > χ^2 = 0.189. The test also finds no heteroscedasticity issues in the relationship between shock sensitivity and $S_{m\mu}$.

The regression analysis in essence plots a best fit line through the data plot, a line that minimizes the sum of squares in the differences between the predicted line Y values and the actual Y values. Table 6 presents the regression output for several specifications. In all of the reported specifications the dependent variable is the level of sensitivity (GPa). The coefficients are reported along with their corresponding t values, included below the coefficient.

Specification I simply examines the impact Rm has on the level of sensitivity of the material. This specification is equivalent to simply plotting the best fit line through the dataset in Figure 1 and is estimated using the HC3 method for the computation of errors. The model can be summarized by the following equation:

$$Sensitivity = 5.998 - 0.153R_m$$

However, the statistical validity of that equation is limited. First, the goodness of fit is low. As measured by the adjusted R-squared, the model explains only about 8% of volatility in the level of sensitivity. Secondly, the coefficient on R_m is statistically significant at only 67%. All the subsequent specifications are estimated without the HC3 technique, as no evidence of heteroscedasticity was found (see the discussion above).

Specification II models Sensitivity as a function of Sm. The level of statistical significance increases substantially. The coefficient on S_m is statistically significant at 99%, suggesting that the level of variation in surface roughness on the surface of the particle has a statistically significant impact on the level of shock sensitivity of the material. Furthermore, the overall goodness of fit of this specification has also improved. The adjusted R-squared suggests that model in Specification II explains over 76% of volatility in sensitivity.

Specification III examines the relationship between $S_{m\mu}$ and sensitivity. The coefficient on $S_{m\mu}$ is statistically significant at 92%. The overall fit of the model is also weaker with the adjusted R-square being at 0.398.

In Specification IV these three measures of surface characteristics are combined into one model. The test for heteroscedasticity failed to reject the hypothesis of homoscedasticity. Thus, the estimation is estimated without the HC3 technique. The overall explanatory power of the model improves substantially with the adjusted R-squared rising to 0.915. The coefficient on R_m is statistically significant at only 67% and the one on $S_{m\mu}$ is statistically significant at 84%, but the coefficient on S_m remains statistically significant at 98%. This specification includes multiple measures of surface characteristics that may in tern be correlated with each other. Although this has already been examined in the correlation table and no meaningful correlation was observed, this is verified with a computation of the variance inflation factor (VIF), see Table 7. The VIF computation confirms what the correlation table suggested, no multicollinearity problems in specification IV.

	Dependent Variable = Sensitivity Specification				
Ind. Vars.	I	II	III	IV	V
Rm	-0.15			-0.04	
	1.07			1.14	
Sm		-0.29		-0.23	
		4.52		5.08	
Smμ			-0.55	-0.23	
			2.23	1.87	
%HMX					-0.05
					0.41
Constant	6.00	6.02	7.26	7.31	4.47
	5.31	14.34	5.41	14.38	8.39
R-sq	0.48	0.80	0.50	0.96	0.03
Adj. R-sq	0.08	0.76	0.40	0.92	-0.16

Table 6. OLS Regression with Heteroscedasticity correction

Variable	VIF	1/VIF
Rm	1.89	0.530049
Smμ	1.81	0.552178
Sm	1.3	0.771688

Table 7. Computation of Variance Inflation Factor.

Specification IV can be written as a simple equation where each coefficient can be interpreted as a partial derivative:

$$Sensitivity = 7.308 - 0.042R_m - 0.225S_m - 0.233S_{m\mu}$$

The last specification examines the relationship between the level of impurity (%HMX) and sensitivity. The regression analysis demonstrates that there is no statistically significant relationship between these two variables. For further analysis of shock sensitivity and its determinants in RDX materials see Bellitto and Melnik (2010) and Bellitto et al (2010).

4. Conclusion

Atomic force microscopy can be used to obtain a large number of data observations at the nanometric level. These data can statistically be used to investigate and establish quantitative relationships between various variables. This work demonstrates that surface characteristics data obtained from topographical scans can be used in investigating the relationship between the shock sensitivity of the materials at the macroscale and their surface roughness characteristics at the nanoscale. Statistical analysis can be used not only to show that there is a statistical relationship, but with the help of regression techniques, can precisely estimate any such relationships. As demonstrated in this chapter, the surface roughness variation on the surface of the particle has a substantial negative impact on the shock sensitivity in RDX materials. A one unit increase in the average standard deviation (S_m) reduces the shock sensitivity by 0.225 GPa. The statistical analysis can also be used to demonstrate absence of any meaningful relationship. For instance, the results demonstrate that the level of HMX impurity does not impact the shock sensitivity in the studied RDX materials.

5. Acknowledgements

This work was supported by the Office of Naval Research (ONR) and the Naval Surface Warfare Center (NSWC) at Indian Head, MD. The authors express their thanks to Mary Sherlock, Robert Raines, Tina Woodland and Philip Thomas for helpful discussions and for providing the samples.

6. References

Doherty, R..M. & Watts, D.S. (2008). Relationship between RDX Properties and Sensitivity. *Propellants, Explosives, Pyrotechnics,* Vol.33, pp. 4-13

Bellitto, V.J. & Melnik M.I. (2010). Surface defects and their role in the shock sensitivity of cyclotrimethylene-trinitramine. *Applied Surface Science,* Vol.256, pp. 3478-3481

Bellitto, V.J.; Melnik, M.I.; Sorensen, D.N. & Chang, J.C. (2010). Predicting the Shock Sensitivity of Cyclotrimethylene-Trinitramine. *Journal of Thermal Analysis and Calorimetery*, Vol. 102, pp. 557-562

Greene, W. H. (2003). *Econometric Analysis*, 5th edition, Prentice Hall,

Levine, D.M.; Stephan, D. F.; Krehbiel, T.C. & Berenson, M.L. (2011). *Statistics for Managers using Microsoft Excel*, 6th edition, Prentice Hall

Long, J.S. & L.H. Ervin (2000). Using Heteroscedasticity Consistent Standard Errors in the Linear Regression Model. *The American Statistician* Vol. 54, pp. 217-224

MacKinnon, J.G. & White, H. (1985). Some heteroskedasticity consistent covariance matrix estimators with improved finite sample properties. *Journal of Econometrics*, Vol . 29, pp. 53-57

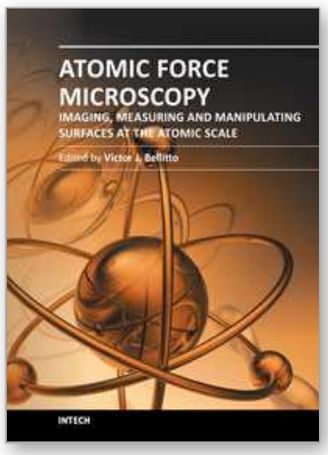

Atomic Force Microscopy - Imaging, Measuring and Manipulating Surfaces at the Atomic Scale

Edited by Dr. Victor Bellitto

ISBN 978-953-51-0414-8
Hard cover, 256 pages
Publisher InTech
Published online 23, March, 2012
Published in print edition March, 2012

With the advent of the atomic force microscope (AFM) came an extremely valuable analytical resource and technique useful for the qualitative and quantitative surface analysis with sub-nanometer resolution. In addition, samples studied with an AFM do not require any special pretreatments that may alter or damage the sample and permits a three dimensional investigation of the surface. This book presents a collection of current research from scientists throughout the world that employ atomic force microscopy in their investigations. The technique has become widely accepted and used in obtaining valuable data in a wide variety of fields. It is impressive to see how, in a short time period since its development in 1986, it has proliferated and found many uses throughout manufacturing, research and development.

InTech Europe
University Campus STeP Ri
Slavka Krautzeka 83/A
51000 Rijeka, Croatia
Phone: +385 (51) 770 447
Fax: +385 (51) 686 166
www.intechopen.com

InTech China
Unit 405, Office Block, Hotel Equatorial Shanghai
No.65, Yan An Road (West), Shanghai, 200040, China
中国上海市延安西路65号上海国际贵都大饭店办公楼405单元
Phone: +86-21-62489820
Fax: +86-21-62489821

IntechOpen